

Behavior of Tar Sand Bitumen With Paraffinic Solvents and Its Application to Separations for Athabasca Bitumen

Edward W. Funk
Exxon Research and Engineering, Linden, N.J., 07036

The main purpose of this paper is to present the behavior of tar sand bitumen when contacted with low-molecular-weight paraffins at ambient temperatures. We have found that an understanding of this phenomenon can lead to new separation and upgrading approaches for Athabasca tar sands. Furthermore, the ideas generated by the study of tar sand bitumen may possibly also be applied to other synthetic fuels such as coal liquids and shale oil.

1. Tar Sand Bitumen Dissolution Using the Spinning Disc Method. The dissolution behavior of tar sand bitumen depends primarily on the solvent, contacting conditions, and the temperature. For studying the dissolution mechanism we have chosen the spinning disc technique as a simple, well-understood system. The spinning disc technique for examining mass transfer and dissolution phenomena is well established in electro-chemistry but can be applied to a variety of systems (1,2). The experimental procedure consists of rotating a circular disc immersed in a liquid at a constant speed. Mass transfer from the disc can be experimentally measured as a function of time and rotational speed. The principal advantage of this geometry is that the mass-transfer coefficient is the same at all points on the surface and can be expressed as

$$k = 0.62 D^{2/3} \nu^{-1/6} \omega^{1/2} \quad 1)$$

where D is the binary diffusion coefficient, ν is the kinematic viscosity and ω is the rotational speed of the disc. The dependence of k on the rotational speed allows separation of mass transfer resistances between phases from resistances within the bulk phase.

For our study, a glass disc 2.54 cm. in diameter was coated with 0.10 grams of tar sand bitumen. The concentration of bitumen in solution was measured using a Beckman DB-G spectrophotometer operating at 530 nm. Details of this analytical technique are given by Funk and Gomez (3).

Figure 1 presents the experimental data for *n*-pentane as the solvent at 25°C. The data were obtained at rotational speeds of 0, 7 and 17 RPM. Figure 1 shows that, over the range of speeds studied, the rate of bitumen dissolution is independent of the rotational speeds. Equation 1 then indicates that the principal resistance to dissolution resides in the bitumen layer and not in transport across the solvent-bitumen interface. This resistance within the bitumen layer is large enough to require several minutes (≈ 10 minutes) for all the deasphalted oil to diffuse out of the bitumen layer.

For a variety of paraffinic solvents, dissolution data were obtained at 25°C and the discs were removed and the remaining asphaltene crust was examined by microscopy. Figure 2 presents SEM photomicrographs for pentane and decane asphaltenes at a magnification of 500. The results show that the asphaltenes form a porous network similar to an alloy which has had one component leached out. For the pentane asphaltenes, the pore size is $\approx 1 \mu$; for decane-precipitated asphaltenes the pores are considerably smaller. Examination of asphaltenes from dissolution using other paraffins showed that the pore size became smaller the higher the carbon number of the paraffinic solvent.

The experimental data can be modeled using Fick's second law which is expressed as

$$\frac{\partial c}{\partial t} = D_{AB} \frac{\partial^2 c}{\partial x^2} \quad 2)$$

To describe the unsteady-state diffusion in the spinning-disc experiments, we use the boundary conditions of $c=c_0$ for $t < 0$ and $c = 0$ in the solvent for all t . Crank (4) gives the solution to Equation 2; the expression for D_{AB} , the binary diffusion coefficient expressing mutual diffusion of solvent and deasphalted oil, is particularly simple at time where one-half of the deasphalted oil has been leached out

$$D_{AB} = \frac{0.049}{(t/L^2)} \quad 3)$$

where L is the thickness of the bitumen layer on the disc. Experimental data consistent with the above model usually show a linear plot of M_t/M_∞ (the fraction of deasphalted oil leached out) versus t^2 over a considerable time range. Figure 3 presents M_t/M_∞ as a function of t^2 for dissolution using pentane, heptane and decane. Equation 3 was used to calculate effective diffusion coefficients from the experimental data. For the pentane system, D_{AB} is 1.41×10^{-7} cm²/sec at 25°C. The results with heptane give a value of D_{AB} of 1.21×10^{-7} cm²/sec and the value for the decane system is 6.50×10^{-9} cm²/sec.

2. Particle Size Analysis of Asphaltene Aggregates. To determine the particle-size distribution of asphaltene aggregates which would be breaking away from the crust, tar sand bitumen was deasphalted using pentane, hexane and heptane at room temperature. The bitumen was contacted with ten times its weight of solvent and the asphaltenes were precipitated using a laboratory centrifuge operating at 2000 RPM. The asphaltenes were washed until they were free of deasphalted oil.

The HIAC model PC-230 was used to measure the particle-size distribution. This instrument uses a light-sensitive diode to determine light attenuation due to particles flowing past the sensor. Figure 4 shows the particle-size distributions for pentane, hexane and heptane precipitated asphaltenes. The results indicate that the pentane asphaltenes are somewhat larger than the hexane asphaltenes; this trend was found consistent through heptane.

3. Structure of Athabasca Tar Sands. For the tar sand system, the bitumen is associated with the sand and water as shown schematically in Figure 5. Typically the Athabasca tar sands contain 12% bitumen, 5% water and 83% sand and other minerals. Details of characterization of tar sands are summarized by Camp (5).

4. Fluid-Bed Studies. A liquid-fluidized bed is a convenient and conventional technique for contacting solids and liquids and we have applied this technique to contact tar sands with paraffinic solvents. Experimental data on the size of asphaltene aggregates for the tar sand system were obtained by using paraffinic solvents to elutriate the asphaltenes from a well-mixed fluidized bed of tar sands. Figure 6 gives a schematic diagram of the equipment used for the elutriation studies. The tar sands were placed in the 2" I.D. glass extraction column and a set of turbine mixers operating at 200 RPM was used to assure good solids-solvent contact. For each run, solvent was passed up through the tar sand bed at a known flowrate and collected at the top of the extraction

column. The extract was then analyzed for the percentage of asphaltenes. Figure 7 presents the results of the elutriation studies at 25°C. The percentage of asphaltenes entrained is expressed relative to the total asphaltenes in the bitumen for the particular paraffinic solvent used. As an example, we expect the extract with pentane to be 20% asphaltenes if all are small enough to be entrained; if the extract is 10% asphaltenes we calculate that only 50% of the asphaltenes were entrained. We see from Figure 7 that liquid flowrates in the range of 1 cm/sec are required to entrain all the asphaltenes with the extracted oil. Consistent with the results shown in Figure 4, the pentane asphaltenes behave as larger particles than the hexane asphaltenes and this trend continues through octane. Figure 8 presents similar data as a function of temperature for heptane as the solvent. As the temperature increases, higher liquid flowrates are required to entrain the asphaltene aggregates and this indicates that the size of the aggregates is increasing. The change in solvent density and viscosity is much too small to account for the higher liquid flowrates.

Use of Stokes' law and the elutriation data shown in Figure 7 were used to calculate effective maximum diameters for the asphaltene aggregates. For heptane, the maximum aggregate diameter is 100 μ and for pentane 150 μ ; these values are somewhat higher than those found using the HIAC particle-size analysis. The difference may be due to the estimated asphaltene density used in the Stokes' law calculation.

5. Novel Approach to Bitumen Separation from Athabasca Tar Sands. We have examined the use of paraffinic solvents for separation of bitumen from tar sands in a fluid bed since this type of contacting equipment has reasonable potential to be scaled up to the very large sizes required for tar sands.

Fluidization data were measured using the equipment shown schematically in Figure 6. For the sample of tar sands used, the particle-size distribution of the inorganics is shown in Figure 9. Figure 10 presents a plot of $\ln U$ versus $\ln \epsilon$ for the tar sand system; these data are for heptane as the solvent and at ambient temperature. The bed shows some expansion at liquid velocities substantially below the minimum fluidization velocity; this is not the case for a bed of equal-sized particles; it probably occurs in the tar sand system due to some segregation of different sized particles to give a fixed-bed region and a fluidized region. The curves A and B for dry tar sands (water removed by evaporation) give an approximate minimum fluidization velocity of the inorganics equal to 1 cm/sec. Curve B simulates the bottom of a hypothetical extractor where the solvent is nearly pure heptane; curve A simulates the other end of the extractor where the solvent has a relatively high bitumen concentration (in this case, heptane/bitumen = 4). The fluidization behavior is very different for fresh water-wet tar sands. These data are shown in Figure 10 by the solid dots. The minimum fluidization velocity is much higher than for dry tar sands. This great difference can be explained by agglomeration of the inorganics in the tar sand bed. Spherical agglomerates are formed in the fluid bed because the water-wet inorganics associate to minimize surface area between water and the hydrocarbon. Details of spherical agglomeration and its application to other systems are given by Smith and Puddington (6).

The results of Figure 10 show that the tar sand inorganics behave like large particles in a fluid bed if care is taken to maintain them as

water-wet. From Figure 7, we know that the asphaltenes behave as relatively small particles. Combining the results of Figures 7 and 10 suggests the conceptual separation approach shown in Figure 11. Figure 11 shows that for a paraffinic solvents there is a range of liquid flowrates which gives carryover of asphaltenes from a fluidized-bed type contactor but does not entrain the inorganics. For example, operating at 1.0 cm/sec to entrain the asphaltenes would entrain an important fraction of the unagglomerated inorganics. Then, a further separation of bitumen from inorganics would be required. The separation shown in Figure 11 is for essentially ambient temperatures.

The results shown in Figure 11 only suggest a conceptual approach for bitumen separation from tar sands. Use of this separation approach on a commercial scale requires considerable process development to generate an integrated system including tar sands preparation, solid-liquid contacting equipment, solids handling, and economic solvent recovery from the extracted tar sands.

6. References

- (1) Levich, V. G., "Physicochemical Hydrodynamics," Prentice-Hall, Inc., Englewood Cliffs, N. J., 1962.
- (2) Chan, A. F., Evans, D. F., and Cussler, E. L., "Explaining Solubilization Kinetics," AIChE Journal 22,1006 (1976).
- (3) Funk, E.W., and Gomez, E., "Determination of Vanadium in Athabasca Bitumen and Other Heavy Hydrocarbons by Visible Spectrometry," Anal. Chem. 49,972 (1977).
- (4) Crank, J., "The Mathematics of Diffusion," Oxford University Press, Second Edition, 1975.
- (5) Camp, F. W., "The Tar Sands of Alberta, Canada," Cameron Engineers, Denver, Colorado, 1969.
- (6) Smith, H. M. and Puddington, I. E., "Spherical Agglomeration of Barium Sulfate," Can. J. Chem., 38, 1911 (1960).

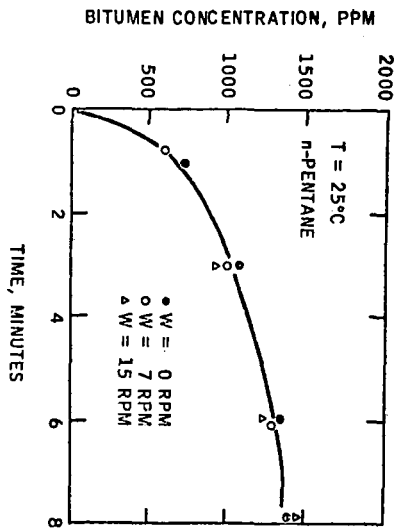
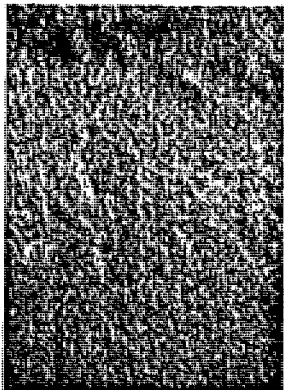


Figure 1 - Spinning Disc Experiments for Tar Sand Bitumen Dissolution in Pentane



Pentane Asphaltenes



Decane Asphaltenes

Figure 2 - Photomicrographs at 500x of Pentane and Decane Asphaltenes

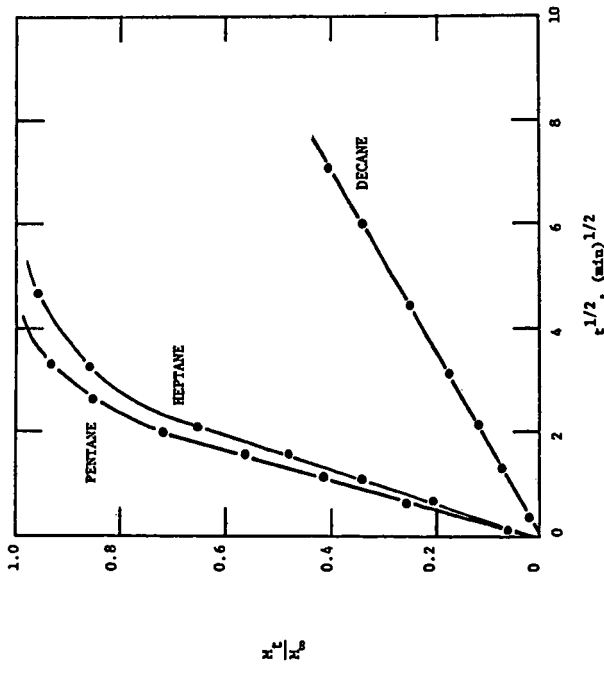


Figure 3 - Bitumen Dissolution in Normal Paraffins

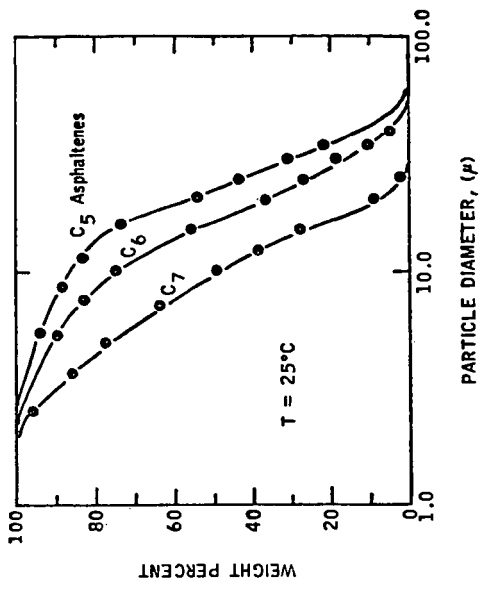


Figure 4 - Particle-Size Distribution of Asphaltene Aggregates

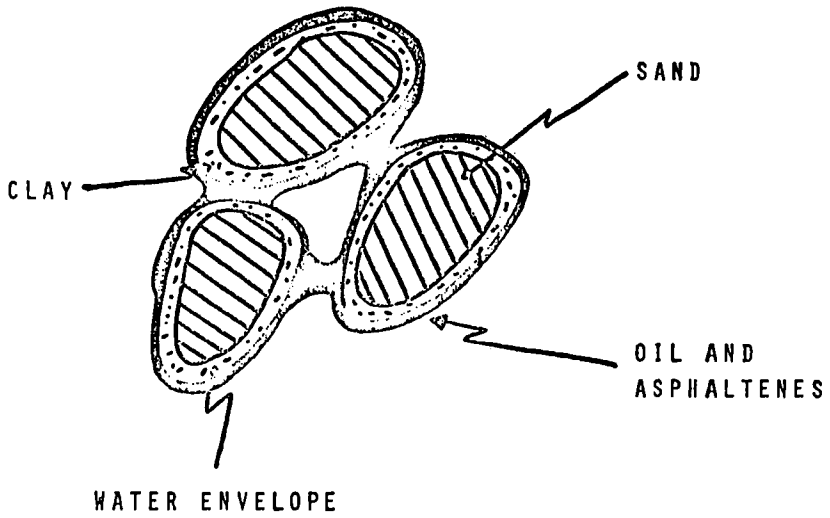


Figure 5 - Basic Model of Athabasca Tar Sands

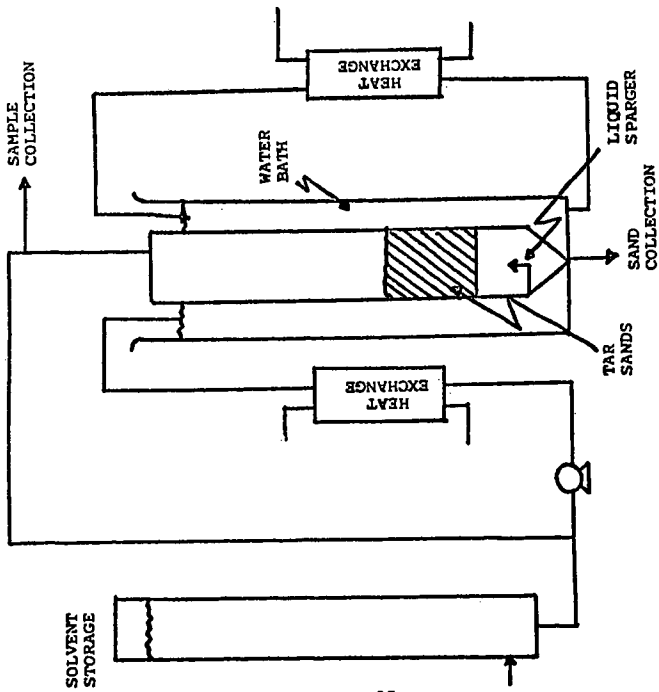


Figure 6 - Schematic Diagram of Fluid-Bed Contactor for Tar Sands

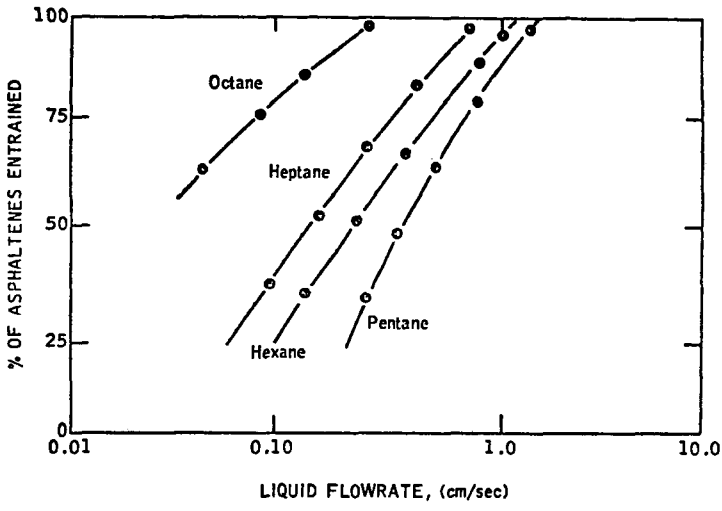


Figure 7 - Entrainment of Asphaltenes from a Tar Sand Bed as a Function of Liquid Velocity

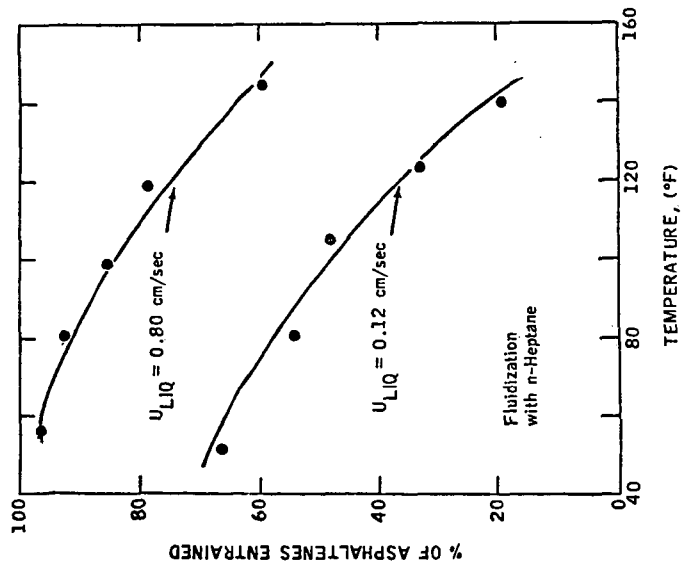


Figure 8 - Effect of Temperature on Entrainment of Asphaltenes from a Fluidized Tar Sand Bed

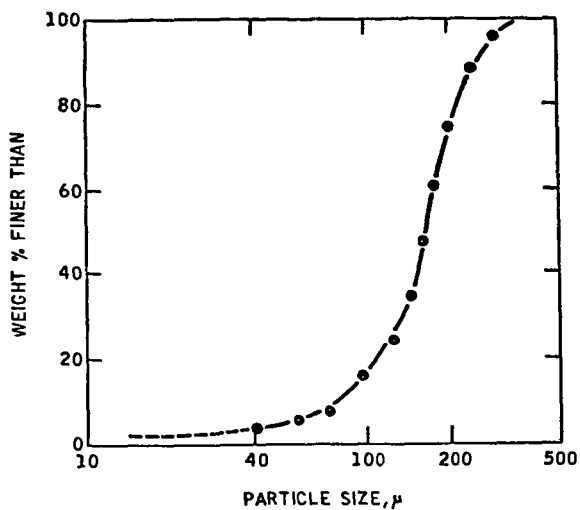


Figure 9 - Typical Particle-Size Distribution of Athabasca Tar Sand Inorganics

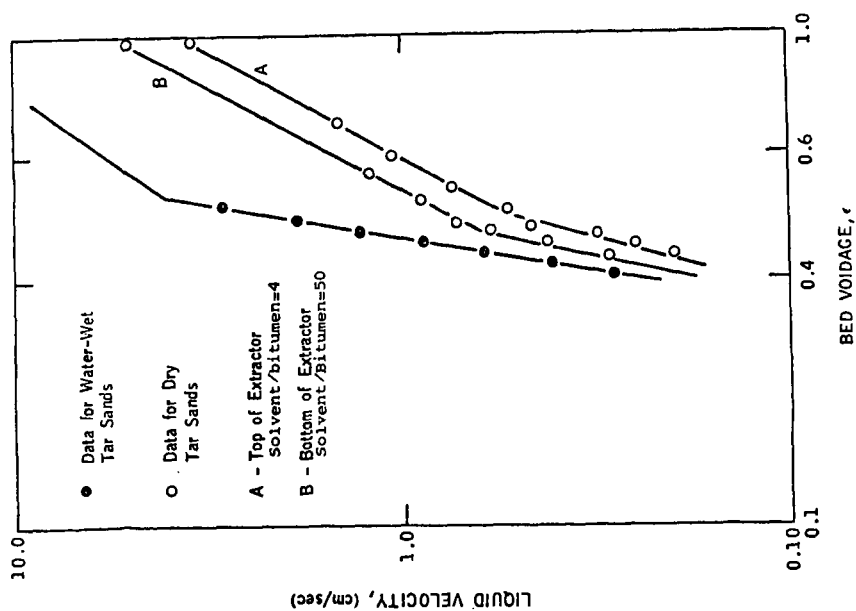


Figure 10 - Fluidization Data for Athabasca Tar Sands with n-Heptane

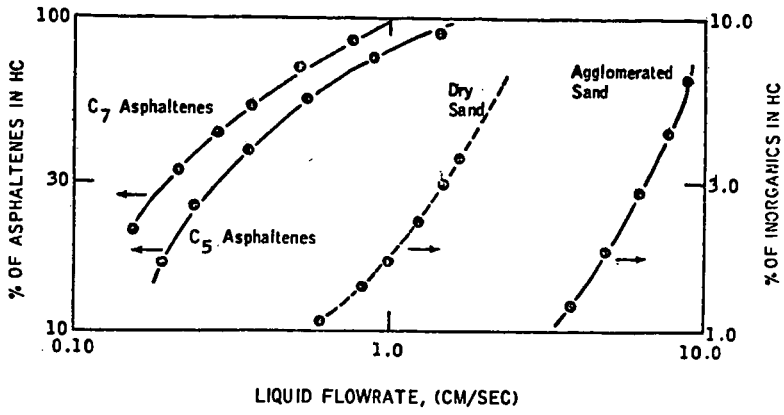


Figure 11 - Conceptual Process for Bitumen Separation from Athabasca Tar Sands